Proceedings of the 2002 IEEE
International Conference on Robotics & Automation
Washington, DC • May 2002

Trajectory design for formations of robots by kinetic energy shaping

Calin Belta and Vijay Kumar

GRASP Laboratory
University of Pennsylvania
Philadelphia, PA 19104
{calin, kumar}@grasp.cis.upenn.edu

Abstract

We develop a method for generating smooth trajectories for a set of mobile robots. Given two end configurations, by tuning one parameter, the user can choose an interpolating trajectory from a continuum of curves varying from that corresponding to maintaining a rigid formation to motion of the robots toward each other. The idea behind our method is to change the original constant kinetic energy metric in the configuration space and can be summarized into three steps. First, the energy of the motion as a rigid structure is decoupled from the energy of motion along directions that violate the rigid constraints. Second, the metric is "shaped" by assigning different weights to each term, and, third, geodesic flow is constructed for the modified metric. The optimal motions generated on the manifolds of rigid body displacements in 3-D space ($SE(3)$) or in plane ($SE(2)$) and the uniform rectilinear motion of each robot corresponding to a totally uncorrelated approach are particular cases of our general treatment.

1 Introduction

Multi-robotic systems are versatile and efficient in exploration missions, surveillance, and cooperative manipulation tasks. Recent research on such systems includes work on cooperative manipulation [9], multi-robot motion planning, mapping and exploration [8], behavior-based formation control [1], and software architectures for multi-robotic systems [10]. We are concerned with the problem of generating optimal trajectories for a team of multiple robots. Most related to our work are the concepts of virtual structures [11], motion planning, and control of space-crafts [2].

This paper builds on our previous work [13, 3, 4]. In [13], minimum energy interpolating trajectories for a rigid body are generated by solving two point boundary value problems on a system of differential equations written in the Lie algebra of $SE(3)$. A computationally efficient approach was suggested in [3]. Geodesics generated in an ambient space $GA(3)$ equipped with an appropriate metric are projected back on $SE(3)$ to generate motion for rigid bodies. This approach leads to a closed form algorithm for robot trajectories, but the solution is only close to the optimal solution. These ideas were extended to robots required to maintain a fixed formation in [4].

The rigid formation constraint is too restrictive in many applications. We would like robots to be able to break formation, cluster together or string themselves out to avoid obstacles, and to regroup to achieve a desired goal formation at the destination. This paper develops a family of trajectories ranging from the trajectories that are optimal for a rigid formation on one extreme to independent trajectories that are optimal for each robot on the other.

We build the geodesic flow of a new metric in the whole configuration space given by collecting the configuration spaces of all robots. This new metric is obtained from the naturally induced (constant) kinetic energy metric dependent on the inertial properties of the robots by first decomposing each tangent space into two metric-orthogonal subspaces and then assigning different weights to the terms corresponding to rigid and non-rigid instantaneous motions. This idea of a "decomposition" and a subsequent "modification" is closely related to the methodology of controlled Lagrangians described in [5, 12]. The optimal motions generated on the manifolds of rigid body displacements in 3-D space ($SE(3)$) or in plane ($SE(2)$) and the uniform rectilinear motion of each robot corresponding to a completely independent approach are also particular cases of our general treatment.

2 Background and problem statement

2.1 Problem formulation

Consider N point-like robots with masses m_i, $i = 1, \ldots, N$ moving in 3-D space with respect to an inertial frame $\{F\}$. The configuration space Q is R^{3N} and a generic configuration $q = (q_1, q_2, \ldots, q_N)$, where q_i is the position vector of robot i in frame $\{F\}$. Given two configurations q^0 and q^1 at times $t = 0$ and $t = 1$ respectively, the goal is to generate smooth interpolating motion for each robot so that the total kinetic energy is minimized while certain constraints on the positions are satisfied. Even though more general problems can be approached, in this paper the focus is on maintaining a rigid

0-7803-7272-7/02/$17.00 © 2002 IEEE

formation (virtual structure) and relaxing the constraint as necessary. This is done by appropriately shaping the kinetic energy metric in the configuration space as described in Section 3. The mathematical tools that we use are outlined in the next section.

2.2 Velocity decomposition

Let Q be the $n+r$ - dimensional configuration space of a system and $\mathcal{G}$ a n - dimensional Lie group that acts on Q so that the Lagrangean defined on TQ is invariant under this action. The state of the system can be described by a pair (g, s), where $g \in \mathcal{G}$ and s is an element in the complementary space $Q/\mathcal{G}$, which we will call the shape space. At any point $q \in Q$, a tangent vector $V_q \in T_qQ$ can be decomposed into a component which is tangent to Orb_q (the orbit of q under actions of $\mathcal{G}$), and a component which is orthogonal (in some metric $<,>$) to this first component (see Figure 1). Following the notation in

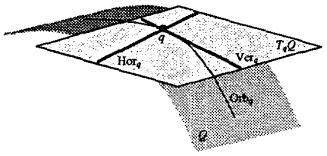

Figure 1: Pointwise decomposition of the tangent space in the vertical and horizontal subspaces

[5, 12], the space $T_q\mathrm{Orb}_q$ is called the vertical space at q, Ver_q, and its orthogonal complement is the horizontal space at $q \in Q$, Hor_q. The decomposition of the tangent vector V_q into $\mathrm{Ver}V_q$ (projection onto Ver_q) and $\mathrm{Hor}V_q$ (projection onto Hor_q) is uniquely defined by requiring that metric $<,>$ satisfies

$$< V_q^1, V_q^2 >=< \mathrm{Hor}V_q^1, \mathrm{Hor}V_q^2 > + < \mathrm{Ver}V_q^1, \mathrm{Ver}V_q^2 >,\ V_q^1,\ V_q^2 \in T_qQ \qquad (1)$$

2.3 The geometry of rigid body motion

Since the rigid bodies (robots) move in three dimensions, the Lie group $\mathcal{G}$ that we are interested in is the special Euclidean group $SE(3)$, the set of all rigid displacements in $\mathbb{R}^3$:

$$SE(3) = \left\{ g \,|\, g = \begin{bmatrix} R & d \\ 0 & 1 \end{bmatrix}, R \in \mathbb{R}^{3\times 3},\ RR^T = I,\ \det R = 1,\ d \in \mathbb{R}^3 \right\}.$$

The Lie algebra of $SE(3)$, denoted by $se(3)$, is given by:

$$se(3) = \left\{ \zeta | \zeta = \begin{bmatrix} \hat{\omega} & v \\ 0 & 0 \end{bmatrix}, \hat{\omega} \in \mathbb{R}^{3\times 3},\ \hat{\omega}^T = -\hat{\omega},\ v \in \mathbb{R}^3 \right\}$$

where $\hat{\omega}$ is the skew-symmetric matrix form of the vector $\omega \in \mathbb{R}^3$. Given a curve $g(t) = (R(t), d(t)) \in SE(3)$ an element $\zeta(t)$ of the Lie algebra $se(3)$ can be associated to the tangent vector $\dot{g}(t)$ at an arbitrary point t by:

$$\zeta(t) = g^{-1}(t)\dot{g}(t) = \begin{bmatrix} \hat{\omega}(t) & R^T\dot{d} \\ 0 & 0 \end{bmatrix} \qquad (2)$$

where $\hat{\omega}(t) = R^T\dot{R}$.

Even though the general results in this paper are formulated for $SE(3)$, the examples are given for $SE(2)$, the Lie group of rigid motions in plane.

Consider a rigid body moving in free space. Assume any inertial reference frame $\{F\}$ fixed in space and a frame $\{M\}$ fixed to the body at point O' as shown in Figure 2. A curve on $SE(3)$ physically represents a motion of the

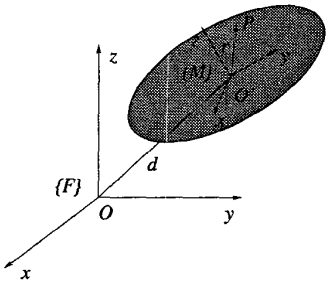

Figure 2: The inertial frame and the moving frame

rigid body. If $\{\omega(t), v(t)\}$ is the vector pair corresponding to $\zeta(t)$, then ω corresponds to the angular velocity of the rigid body while v is the linear velocity of O', both expressed in the frame $\{M\}$. In kinematics, elements of this form are called twists and $se(3)$ thus corresponds to the space of twists. The twist $\zeta(t)$ computed from Equation (2) does not depend on the choice of the inertial frame $\{F\}$.

If P is an arbitrary point on the rigid body with position vector r in frame $\{M\}$ (Figure 2), then the velocity of P in frame $\{M\}$ is given by

$$v_P = \begin{bmatrix} -\hat{r} & I_3 \end{bmatrix}\zeta \qquad (3)$$

where ζ is the twist of the rigid body.

2.4 The left invariant kinetic energy metric

For a rigid system of N particles with masses $m_1, \ldots, m_N$ and position vectors $r_1, \ldots, r_N$ in the body fixed frame $\{M\}$, the matrix of the (left invariant) kinetic energy metric on $SE(3)$ is [4]:

$$\mathcal{M} = \begin{bmatrix} -\sum_{i=1}^N m_i\hat{r}_i^2 & \sum_{i=1}^N m_i\hat{r}_i \\ -\sum_{i=1}^N m_i\hat{r}_i & \sum_{i=1}^N m_i I_3 \end{bmatrix} \qquad (4)$$

and the kinetic energy is given by $1/2\zeta^T\mathcal{M}\zeta$, where $\zeta \in se(3)$ is the (left invariant) twist. The upper left 3×3 submatrix of $\mathcal{M}$ is the inertia matrix of the system of particles with respect to $\{M\}$. If frame $\{M\}$ is placed at the center of mass and aligned with the principal axes of the structure, then $\mathcal{M}$ becomes diagonal.

3 Shaping the kinetic energy

The metric $<,>$ that we define in the configuration space is the same at all points $q \in Q$:

$$< V_q^1, V_q^2 >= {V_q^1}^T M V_q^2, \qquad (5)$$

$$V_q = \dot{q} \in T_qQ, \;\; M = \frac{1}{2}\mathrm{diag}\{m_1 I_3, \ldots, m_N I_3\}$$

Metric (5) is called the *kinetic energy metric* because its induced norm ($V_q^1 = V_q^2 = \dot{q}$) assumes the familiar expression of the total kinetic energy of the system $1/2 \sum_{i=1}^{N} m_i \dot{q}_i^T \dot{q}_i$.

The geodesic for metric (5) is obviously a straight line uniformly parameterized in time interpolating between q^0 and q^1 in Q. By shaping the metric, we mean smoothly changing the metric at T_qQ so that motion along some specific directions is allowed while motion along some other directions is penalized. The new metric will no longer be constant - the Christoffel symbols of the corresponding symmetric connection will be non-zero. The associated geodesic flow gives optimal motion.

3.1 Motion decomposition: rigid vs. non-rigid

In this paper, the Lie group $\mathcal{G}$ as defined in Section 2.2 is $SE(3)$. The left action of $\mathcal{G}$ on Q is the rigid body displacement applied to each q_i written in homogeneous form. The $\mathcal{G}$-orbit at q is the set of all poses that the structure $(q_1, q_2, \ldots, q_N)$ can reach if it was assumed rigid at some instant with $\{M\} \equiv \{F\}$. At each point in the configuration space, in the corresponding tangent space, the velocity corresponding to infinitesimal rigid motion is given by $\mathrm{Ver}V_q$. Therefore, Ver_q locally describe the set of all rigid body motion directions. The orthogonal complement to Ver_q, Hor_q will be the set of all directions violating the rigid body constraints.

Using (3), it is easy to see that Ver_q is the range of the following $3N \times 6$ matrix:

$$\mathrm{Ver}_q = \mathrm{Range}(A(q)), \;\; A(q) = \begin{bmatrix} -\hat{q_1} & I_3 \\ \ldots & \ldots \\ -\hat{q_N} & I_3 \end{bmatrix} \qquad (6)$$

The coordinates of the expansion of $\mathrm{Ver}V_q \in \mathrm{Ver}_q$ along the columns of $A(q)$ are exactly the components of the left invariant twist $\zeta \in se(3)$ of the virtual structure formed by $(q_1, \ldots, q_N)$ and $\{M\} \equiv \{F\}$ at that instant: $\mathrm{Ver}V_q = A\zeta$. Using metric (5), the orthogonal complement of Ver_q is

$$\mathrm{Hor}_q = \mathrm{Null}(A(q)^T M) \qquad (7)$$

Let $B(q)$ denote a matrix whose columns are a basis of Hor_q. Let ψ denote the components of $\mathrm{Hor}V_q$ in this basis: $\mathrm{Hor}V_q = B(q)\psi$. Therefore, the velocity at point q can be written as:

$$V_q = \mathrm{Ver}V_q + \mathrm{Hor}V_q = A(q)\zeta + B(q)\psi \qquad (8)$$

Then, requirement (1) is satisfied. Indeed,

$$\begin{aligned} < V_q^1, V_q^2 >= {V_q^1}^T M V_q^2 = {\zeta^1}^T A^T M A \zeta^2 + \\ + {\zeta^1}^T A^T M B \psi^2 + {\psi^1}^T B^T M A \zeta^2 + {\psi^1}^T B^T M B \psi^2 = \\ = {\zeta^1}^T A^T M A \zeta^2 + {\psi^1}^T B^T M B \psi^2 = \\ =< B\psi^1, B\psi^2 > + < A\zeta^1, A\zeta^2 >= \\ =< \mathrm{Hor}V_q^1, \mathrm{Hor}V_q^2 > + < \mathrm{Ver}V_q^1, \mathrm{Ver}V_q^2 > \end{aligned}$$

because both $A^T M B$ and $B^T M A$ are zero from (7). Also, note that

$$\begin{aligned} \zeta &= (A^T M A)^{-1} A^T M V, \\ \psi &= (B^T M B)^{-1} B^T M V \end{aligned} \qquad (9)$$

Therefore, the kinetic energy (which is the square of the norm induced by metric (5)) becomes:

$$K(q, \dot{q}) = \dot{q}^T M \dot{q} = \zeta^T A^T M A \zeta + \psi^T B^T M B \psi \quad (10)$$

Straightforward calculation shows that $A^T M A$ is the same as (4), (when $r_i = q_i$, $\{M\} = \{F\}$) *i.e.*, the matrix of the left invariant kinetic energy metric if the system of particles is assumed rigid.

3.2 Metric shaping

In (10), $\zeta^T A^T M A \zeta$ captures the energy of the motion of the system of particles as a rigid body, while the remaining part $\psi^T B^T M B \psi$ is the energy of the motion that violates the rigid body restrictions. For example, in the obvious case of a system of $N = 2$ particles, the first part corresponds to the motion of the two particles connected by a rigid massless rod, while the second part would correspond to motion along the line connecting the two bodies. In this paper, we "shape" the original metric (5)) by putting different weights on the terms corresponding to the rigid and non-rigid motions:

$$\begin{aligned} < V_q^1, V_q^2 >_\alpha = \alpha < \mathrm{Hor}V_q^1, \mathrm{Hor}V_q^2 > + \\ (1-\alpha) < \mathrm{Ver}V_q^1, \mathrm{Ver}V_q^2 > \end{aligned} \qquad (11)$$

Using (9) to go back to the original coordinates, we get the modified metric in the form:

$$< V_q^1, V_q^2 >_\alpha = {V_q^1}^T M_\alpha(q) V_q^2, \qquad (12)$$

where the new matrix of the metric is now dependent on the artificially introduced parameter α and the point on the manifold $q \in Q$:

$$\begin{aligned} M_\alpha(q) = \alpha M A (A^T M A)^{-T} A^T M + \\ (1-\alpha) M B (B^T M B)^{-T} B^T M \end{aligned} \qquad (13)$$

The influence of the parameter α can be best seen by examining the significance of α taking on the values of 0, 0.5 and 1. The two extreme values of α, 0 and 1, cause the metric (12) to become singular. $\alpha = 1$ reduces to the

rigid formation metric (4) on $\mathcal{G}$, while $\alpha = 0$ yields a metric for motions along the fiber $Q/\mathcal{G}$. The intermediate case, $\alpha = 0.5$, yields the kinetic energy of a system of independent robots.

As α tends to 0, the preferred motions will be ones where robots cluster together through much of the duration of the trajectory, thus minimizing the *rigid body energy* consumption. As α approaches 0.5, the motions degenerate toward uncoordinated, independent motions. As α tends to 1, the preferred motions are ones where the robots stay in rigid formation through most of the trajectory, thus minimizing the energy associated with *deforming* the formation.

4 Trajectory generation

We use the geodesic flow of metric (12) to produce smooth interpolating motion between two given configurations:

$$q^0 = q(0), \quad q^1 = q(1) \in \mathbb{R}^{3N} \tag{14}$$

To simplify the notation, let x_i, $i = 1, \ldots, 3N$ denote the coordinates $q_i \in \mathbb{R}^3$, $i = 1, \ldots, N$ on the configuration manifold Q. In this coordinates, the geodesic flow is described by the following differential equations [6]:

$$\ddot{x}_i + \sum_{j,k} \Gamma^i_{jk} \dot{x}_j \dot{x}_k = 0, \; i = 1, \ldots, 3N \tag{15}$$

where Γ^k_{ij} are the Christoffel symbols of the unique symmetric connection associated to metric (12):

$$\Gamma^k_{ij} = \frac{1}{2} \sum_h \left(\frac{\partial m_{hj}}{\partial x^i} + \frac{\partial m_{ih}}{\partial x^j} - \frac{\partial m_{ij}}{\partial x^h} \right) m^{hk} \tag{16}$$

m_{ij} and m^{ij} are elements of M_α and M_α^{-1}, respectively. Because $\alpha = 0$ and $\alpha = 1$ make the metric singular, (16) can only be used for $0 < \alpha < 1$.

5 Example: two bodies in the plane

Consider two bodies of masses m_1 and m_2 moving in the $x - y$ plane. The configuration space is $Q = R^4$ with coordinates $q = [x_1, y_1, x_2, y_2]^T$. The symmetry group $\mathcal{G}$ is the three-dimensional $SE(2)$. The A and B matrices describing Ver_q and Hor_q as in (6) and (7) are:

$$A = \begin{bmatrix} -y_1 & 1 & 0 \\ x_1 & 0 & 1 \\ -y_2 & 1 & 0 \\ x_2 & 0 & 1 \end{bmatrix}, \quad B = \begin{bmatrix} \frac{m_2(x_2 - x_1)}{m_1(y_1 - y_2)} \\ -\frac{m_2}{m_1} \\ \frac{x_1 - x_2}{y_1 - y_2} \\ 1 \end{bmatrix}$$

The 64 Christoffel symbols $\Gamma^k = (\Gamma^k_{ij})_{ij}$ of the connection associated with the modified metric at $q \in Q$ become:

$$\Gamma^1 = \frac{2(1-2\alpha)}{\alpha} \frac{m_2}{m_1 + m_2} \frac{d_x}{(d_x^2 + d_y^2)^2} \Gamma$$

$$\Gamma^2 = \frac{2(1-2\alpha)}{\alpha} \frac{m_2}{m_1 + m_2} \frac{d_y}{(d_x^2 + d_y^2)^2} \Gamma$$

$$\Gamma^3 = -\frac{2(1-2\alpha)}{\alpha} \frac{m_1}{m_1 + m_2} \frac{d_x}{(d_x^2 + d_y^2)^2} \Gamma$$

$$\Gamma^4 = -\frac{2(1-2\alpha)}{\alpha} \frac{m_1}{m_1 + m_2} \frac{d_y}{(d_x^2 + d_y^2)^2} \Gamma$$

where

$$\Gamma = \begin{bmatrix} -d_y^2 & d_x d_y & d_y^2 & -d_x d_y \\ d_x d_y & -d_x^2 & -d_x d_y & d_x^2 \\ d_y^2 & -d_x d_y & -d_y^2 & d_x d_y \\ -d_x d_y & d_x^2 & d_x d_y & -d_x^2 \end{bmatrix}$$

and $d_x = x_1 - x_2$, $dy = y_1 - y_2$. It can be easily seen that, as expected, all Christoffel symbols are zero if $\alpha = 0.5$. Also, the actual masses of the robots are not relevant, it's only the ratio m_1/m_2 which is important.

In this example, we assume $m_2 = 2m_1$ and the boundary conditions:

$$q^0 = \begin{bmatrix} 1 \\ 0 \\ -0.5 \\ 0 \end{bmatrix}, \quad q^1 = \begin{bmatrix} 3 - \frac{\sqrt{2}}{2} \\ -\frac{\sqrt{2}}{2} \\ 3 + \frac{\sqrt{2}}{4} \\ \frac{\sqrt{2}}{4} \end{bmatrix}$$

which correspond to a rigid body displacement so that we can compare our results to the optimal motion corresponding to a rigid body. If the structure was assumed rigid, then the optimal motion is described by uniform rectilinear translation of the center of mass between $(0, 0)$ and $(3, 0)$ and uniform rotation between 0 and $3\pi/4$ around $-z$ placed at the center of mass. The corresponding trajectories of the robots are drawn in solid line in all the pictures in Figure 3. It can be easily seen that there is no difference between the optimal motion of the virtual structure solved on $SE(2)$ and the geodesic flow of the modified metric with $\alpha = 0.99$ (Figure 3, bottom). If $\alpha = 0.5$, all bodies move in straight line as expected (Figure 3, middle). For $\alpha = 0.2$, the bodies go toward each other first, and then split apart to attain the final positions (Figure 3, top).

6 Example: three bodies in the plane

The calculation of the trajectories for three bodies moving in the plane is simplified by assuming that the robots are identical, and, without loss of generality, we assume $m_1 = m_2 = m_3 = 1$. The vertical and the horizontal spaces at a generic configuration

$$q = [x_1, y_1, x_2, y_2, x_3, y_3]^T \in Q = \mathbb{R}^6$$

are given by

$$\mathrm{Ver}_q = \mathrm{Range}(A), \; A = \begin{bmatrix} -y_1 & 1 & 0 \\ x_1 & 0 & 1 \\ -y_2 & 1 & 0 \\ x_2 & 0 & 1 \\ -y_3 & 1 & 0 \\ x_3 & 0 & 1 \end{bmatrix},$$

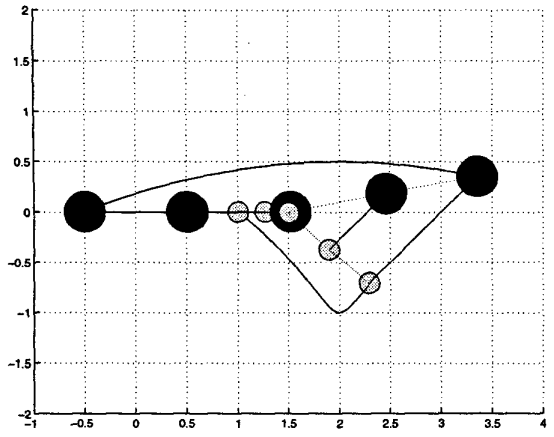

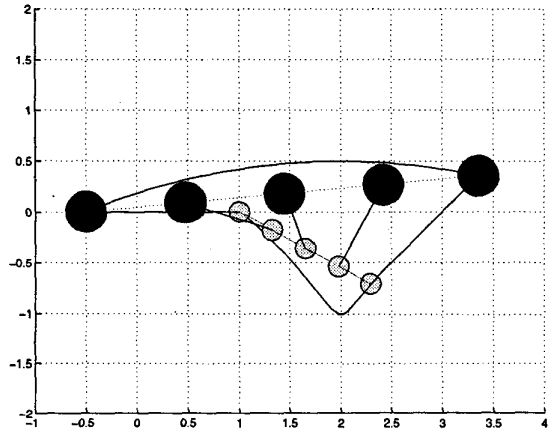

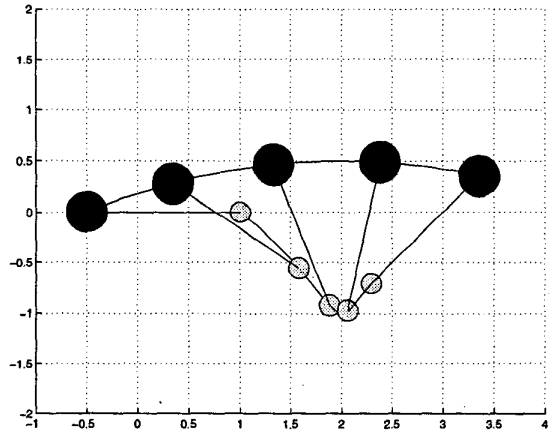

Figure 3: Three interpolating motions for a set of two planar robots as geodesics of a modified metric defined in the configuration space.

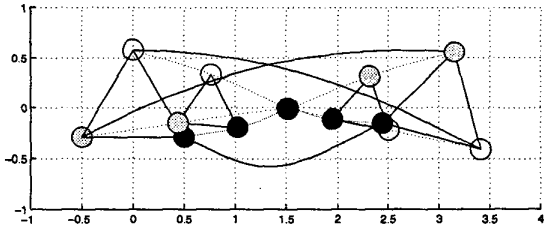

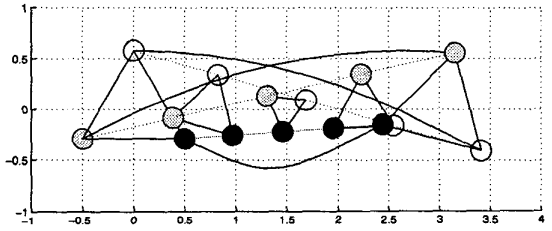

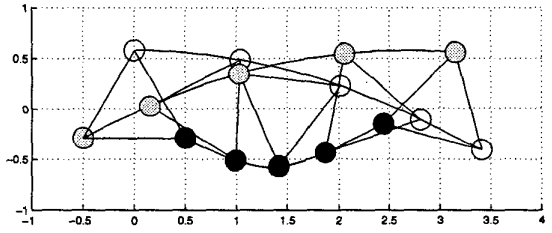

Figure 4: Three interpolating motions for a set of three planar robots as geodesics of a modified metric defined in the configuration space.

$$\mathrm{Hor}_q = \mathrm{Range}(B),\ B = \begin{bmatrix} \frac{x_3-x_1}{y_1-y_2} & \frac{y_2-y_3}{y_1-y_2} & \frac{x_2-x_1}{y_1-y_2} \\ -1 & 0 & -1 \\ \frac{x_1-x_3}{y_1-y_2} & \frac{y_3-y_1}{y_1-y_2} & \frac{x_1-x_2}{y_1-y_2} \\ 0 & 0 & 1 \\ 0 & 1 & 0 \\ 1 & 0 & 0 \end{bmatrix}$$

For simplicity, we omit the expressions of the modified metric and of the Christoffel symbols. The simulation scenario resembles the one in Section 5: the end poses correspond to a rigid structure consisting of a equilateral triangle with side equal to 1. The optimal trajectory solved on $SE(2)$ corresponds to rectilinear uniform motion of the center of mass (line between (0,0) and (3,0) in Figure 4) and uniform rotation from angle 0 to $3\pi/4$ around axis $-z$. The resulting motion of each robot is shown solid, while the actual trajectory for the corresponding value of α is shown dashed. First note for $\alpha = 0.99$ the trajectories are basically identical with the optimal traces produced by the virtual structure, as expected. In the case $\alpha = 0.5$ the bodies move in straight line (corresponding to the unmodified metric). The tendency to cluster as α decreases is seen for $\alpha = 0.2$. Note also that due to our choice $m_1 = m_2 = m_3$, the geometry of the equilateral triangle is preserved for all values of α, it only scales down when α decreases from 1.

7 Conclusion and future work

We presented a strategy for generating a family of smooth interpolating trajectories for a team of mobile robots. The family is parameterized by a scalar α. As α becomes closer to zero, the robots will tend to cluster together while moving between initial and final positions. The case $\alpha = 0.5$ corresponds to a totally uncoordinated strategy: each robot will move from its initial to its final position while minimizing its own energy. Finally, as α tends to 1, the robots try to preserve the distances between them and minimize the overall energy of the motion. This constitutes an alternative to generating motion for virtual structures by solving an optimization problem on the manifold of rigid body displacements $SE(3)$ [4].

While the paper provides a useful conceptual framework for motion planning and generation of trajectories, there is a practical limitation to this work. As the number of robots, n, increases, the generation of the Christoffel symbols and the solution of the two-point boundary value problem become more complicated.

To overcome this difficulty, we plan to develop an alternative description of the shape of the formation, which is independent of the exact coordinates of the robots. This would allow the designer to focus on the gross motion $g \in \mathcal{G}$ and the shape $r \in \mathcal{R}$, while the control of the robots to maintain the prescribed shape r can be done at a lower level of control.

References

[1] Balch, T., and Arkin, R.C., "Behavior-based formation control for multi-robot teams", IEEE Trans on Robotics and Autom, vol.14, no.6, pp.1-15, 1998.

[2] Beard, R.W., and Hadaegh, F.Y., "Constellation templates: an approach to autonomous formation flying", World Automation Congress, Anchorage, Alaska, 1998.

[3] Belta, C., and Kumar, V., "New metrics for rigid body motion interpolation", Ball 2000 Symposium, University of Cambridge, UK, 2000.

[4] Belta, C., and Kumar, V., "Motion generation for formations of robots: a geometric approach", IEEE Int. Conf. Robot. Automat., Seoul, Korea, 2001.

[5] Bloch, A.M., Leonard, N.E., and Marsden, J.E., "Controlled Lagrangians and the stabilization of mechanical systems I: the first matching theorem", IEEE Transactions on Automatic Control, vol.45, no.12, 2000.

[6] do Carmo, M.P., "Riemannian geometry",Birkhauser, Boston, 1992.

[7] Desai, J.P., Ostrowski J.P., and Kumar, V., "Controlling formations of multiple mobile robots", Proc. IEEE Int. Conf. Robot. Automat., pp.2864-2869, Leuven, Belgium, 1998.

[8] Fox, D., Burgard, W., Kruppa, H., and Thrun, S., "Collaborative multi-robot exploration", Autonomous Robots, vol.8, no.3, 2000.

[9] Kang, W., Xi, N., and Sparks, A., "Formation control of autonomous agents in 3D workspace", Proc. IEEE Int. Conf. Robot. Automat., pp. 1755-1760, San Francisco, CA, 2000.

[10] Parker, L. E., "Current state of the art in distributed robot systems", Distributed Autonomous Robotic Systems, Springer, pp. 3-12, 2000.

[11] Tan, K., and Lewis, M.A., "Virtual structures for high-precision cooperative mobile robot control", Autonomous robots, vol.4, no.4, pp.387-403, 1997.

[12] Woolsey, C.A., Bloch, A.M., Leonard, N.E., and Marsden, J.E., "Physical dissipation and the method of controlled Lagrangians", European control conference, 2001.

[13] Žefran, M., Kumar, V., and Croke, C., "On the generation of smooth three-dimensional rigid body motions", IEEE Transactions on Robotics and Automation, vol.14(4), pp.579–589, 1995.